Quantitative retrieval of the angular dependence of laser-induced electron rescattering in molecules

Hongtao Hu [1], Sarayoo Kangaparambi,[1] Martin Dorner-Kirchner [1], Václav Hanus [1], Andrius Baltuška,[1]
Markus Kitzler-Zeiler [1], and Xinhua Xie (谢新华) [1,2,*]

[1]*Photonics Institute, Technische Universität Wien, A-1040 Vienna, Austria*
[2]*SwissFEL, Paul Scherrer Institute, 5232 Villigen PSI, Switzerland*

We demonstrate a time-domain method to quantitatively retrieve the angular dependence of laser-induced electron rescattering from the measured rotational half-revival signals of molecules with a reaction microscope. The method is based on the measured channel-resolved ion yields of single ionization and electron-rescattering-induced double ionization and the *in situ* measured alignment distribution of molecules. From the measured data for CO_2, we retrieve the angular dependence of electron rescattering in nonsequential double ionization for both nondissociative and dissociative cases. The results imply that the angular dependence of electron rescattering is affected by the state of the parent ion populated during the first ionization step. The method demonstrated here opens up the possibility to quantitatively retrieve from measured data which molecular orbitals are involved in the interaction of strong laser fields with molecules.

I. INTRODUCTION

Laser-induced electron rescattering is an essential step in many processes in attosecond science ranging from high-order harmonic generation to laser-induced electron diffraction [1–3]. For molecules, the geometry and the alignment with respect to the laser polarization direction plays an important role in laser-induced molecular dynamics including electron rescattering [4–14]. So far, in the application of high harmonic spectroscopy and tomography of molecules, the rescattering electron wave packets are mainly treated as plane waves [15–18]. Knowledge on the angular dependence of electron rescattering is necessary to achieve a better understanding of electron-rescattering-related strong-field processes in molecules.

Nonsequential double ionization (NSDI) is a typical electron-rescattering-induced process in atoms and molecules during interaction with strong laser fields [19–22], which can therefore be exploited to study the angular dependence of electron scattering. In molecules, not only the first ionization step but also the electron rescattering depends on the molecular alignment. Previous studies on the dependence of high-order harmonic generation and ionization on molecular alignment exclusively focused on the ionization step [5–11]. In comparison with ionization, direct access to the angular dependence information of electron rescattering is not trivial. Previously, angular dependence of laser-induced electron rescattering was investigated based on the measured ion yields as a function of the angle between the laser field polarization and the molecular axis of prealigned molecules [23,24]. In these approaches, the retrieved angular dependence strongly relies on the quality of molecular alignment and also in-

cludes the systematic errors from the measurement of the polarization angle. In the present work, we demonstrate a robust time-domain method for quantitatively retrieving the angular dependence of laser-induced electron rescattering of molecules from channel-resolved rotational half-revival signals of single and double ionization. Our method rules out the influence of the alignment quality with the *in situ* measured molecular alignment distribution and therefore provides a more quantitatively accurate angular dependence than previous approaches. Using CO_2 as an example, we measured ion yields of single and double ionization around the rotational half revival of the laser-induced field-free alignment with a reaction microscope. From the measured time-domain signals, we obtained the angular dependence of single and double ionization by deconvolution of the half-revival signal with the *in situ* measured molecular alignment distribution through a fitting procedure. For both nondissociative and dissociative NSDI, we furthermore retrieved the angular dependence of electron rescattering using the measured angular dependence of single and double ionization as a reference.

II. EXPERIMENTS

In the experiment, we used a reaction microscope for coincidence detection of electrons and ions produced from the interaction of CO_2 molecules with strong laser pulses [25–27], as shown in Fig. 1(a). Linearly polarized laser pulses were delivered from a home-built femtosecond Ti:sapphire amplifier with a central wavelength of 795 nm, a full-width-at-half-maximum pulse duration of 30 fs, and a repetition rate of 5 kHz. The laser beam from the amplifier was split into two arms. The pulses in one arm were used to prealign the CO_2 molecules with a peak intensity of below $10^{14}\,\mathrm{W/cm^2}$ on target [28,29]. The pulses in the second arm were focused to a peak intensity of higher than $10^{14}\,\mathrm{W/cm^2}$ and induced

---

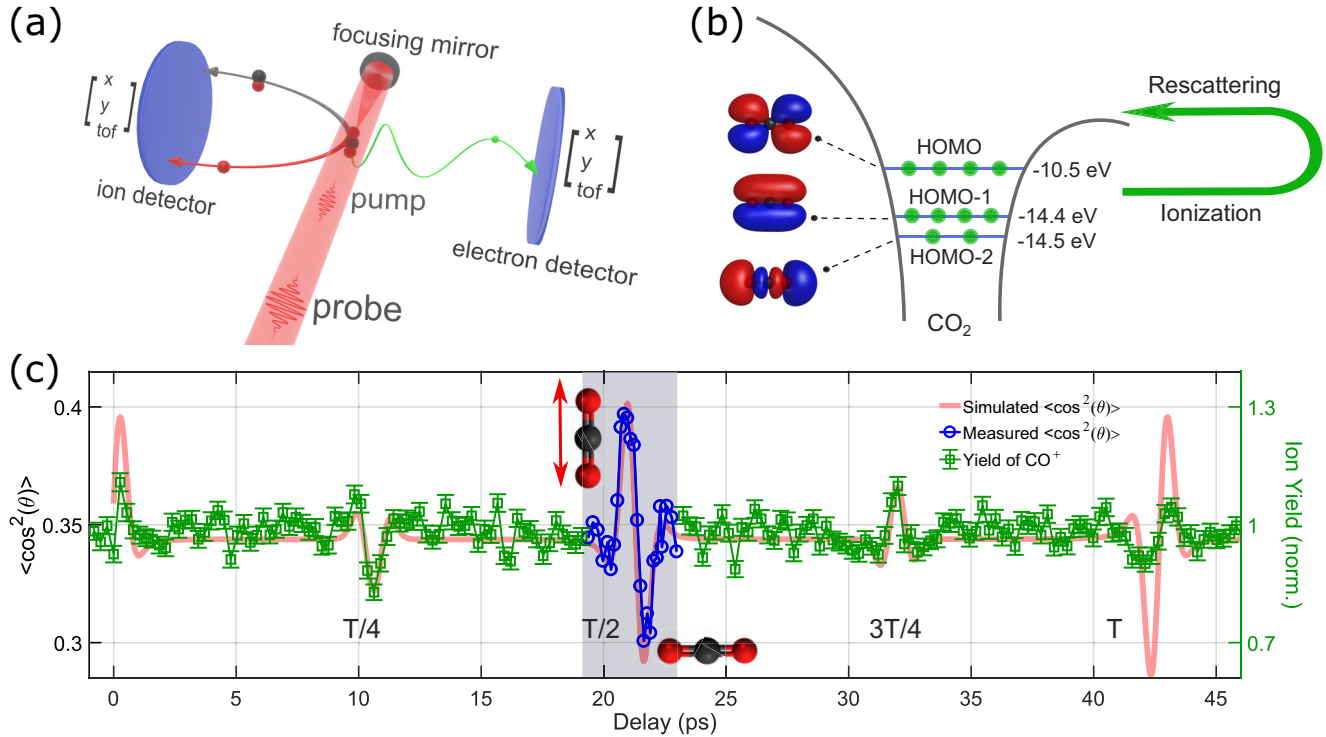*Corresponding author: xinhua.xie@psi.ch

FIG. 1. (a) Schematic view of experimental setup. (b) Schematic view of the laser-induced electron-rescattering process and the involved molecular orbitals of CO_2. (c) Measured CO^+ signal normalized by its mean value (green squares with error bars) from channel 3 as a function of the time delay between the alignment and the ionization pulse. Around the half revival ($\sim$19–23 ps), blue circles present measured $\langle \cos^2 \theta \rangle$. Simulated $\langle \cos^2 \theta \rangle$ is plotted as a solid red line. The red double arrow indicates the laser polarization direction.

strong field ionization and molecular dynamics. The time delay between the two beams was controlled through a linear delay stage with a step size of 13.3 fs. With the reaction microscope we obtained the three-dimensional momentum vectors of resulting particles from the laser-molecule interaction. Measured CO^+ signals as a function of the time delay between the alignment pulse and the ionization pulse are depicted in Fig. 1(c), which shows the evolution of the rotational excitation triggered by the alignment pulse with quarter, half, and full revivals at 11.5, 21, and 42 ps [30]. For retrieving the angular dependence of strong-field processes, we performed measurements in the time window of 19 to 23 ps around the half revival of the molecule. For the measurements, we chose a laser peak intensity of 1.5×10^{14} W/cm^2 for the second pulse, for which NSDI induced by electron rescattering dominates the double-ionization process [20]. The laser peak intensity was calibrated using the measured proton energy distribution from H_2 [31].

III. RESULTS AND DISCUSSIONS

From the measurements, we identified five significant channels after single and double ionization of CO_2 through time-of-flight selection for channels with one charged ion and photoion-photoion coincidence selection for channels with two charged ions [32], which are summarized as follows with the branching ratios in parentheses:

(1) $CO_2 \rightarrow CO_2^+ + e$ (92.6%).
(2) $CO_2 \rightarrow CO_2^{2+} + 2e$ (0.7%).
(3) $CO_2 \rightarrow CO^+ + O + e$ (4.3%).

(4) $CO_2 \rightarrow CO + O^+ + e$ (2.0%).
(5) $CO_2 \rightarrow CO^+ + O^+ + 2e$ (0.4%).

Channels 1, 3, and 4 result from single ionization, while channels 2 and 5 result from double ionization though electron rescattering following single ionization. To achieve a decent signal-to-noise ratio, for each delay point we measured for 240 s with 1.2×10^6 laser shots. Figures 2(a) and 2(b) present the normalized yield of channels 1–5 as a function of the time delay between the alignment pulse and the ionization pulse around the rotational half revival of CO_2. We acquired the molecular axis distribution of molecules $A(\theta, t)$, with θ the angle between the molecular axis and the laser polarization direction, from the Coulomb explosion of channel 5 with the molecular axis defined by the momentum vector of ejected cations in the laboratory frame, shown in Fig. 1(c) as blue circles around the rotational revival. The distribution indicates that CO_2 molecules are aligned preferentially parallel to the laser polarization at the delay of 21 ps while perpendicular alignment is dominant at 21.6 ps. In Fig. 1(c) the simulated values (the red line) were obtained by simulating the molecular rotation dynamics by solving the time-dependent Schrödinger equation [33] with a polarizability orthogonal to the molecular axis of 1.95 Å^3 and an anisotropy of 2.0 Å^3 [34], and a rotational constant of 0.39 cm^{-1} [35]. The molecular temperature and the peak intensity of the alignment pulse were determined to be 70 K and 2.5×10^{13} W/cm^2 to achieve the best agreement with the measured signals. Earlier studies revealed that the dependence of the ionization signal on the time delay between the alignment pulse and the ionization pulse is determined by the alignment distribution and the
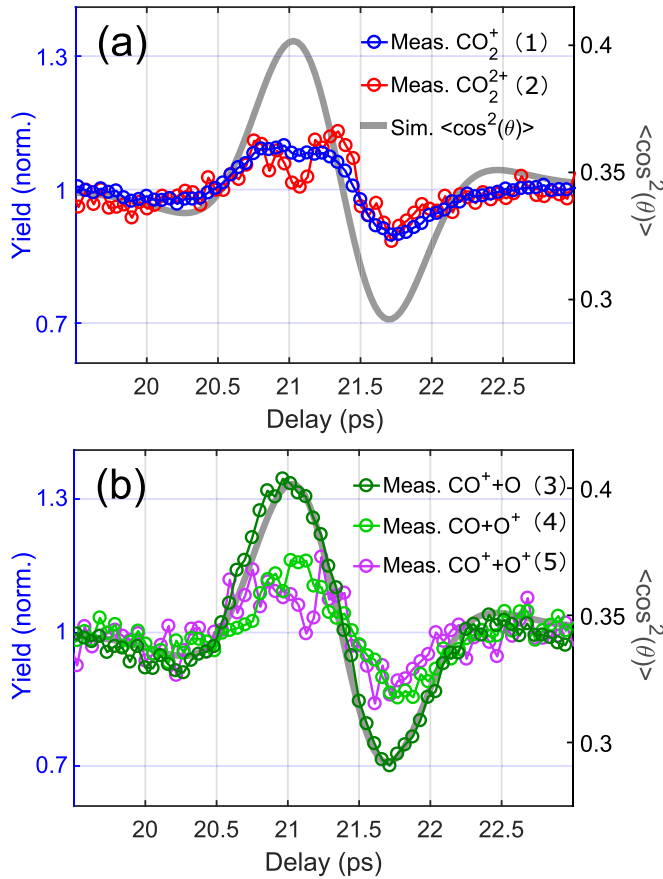
FIG. 2. Measured ion yields for (a) channels 1 and 2 and (b) channels 3–5 as a function of the time delay between the alignment and the ionization pulse in the half revival range. All yields are normalized to the mean yield of the corresponding channel. The gray lines are simulated $\langle \cos^2 \theta \rangle$ representing the alignment of CO_2 molecules.

angular-dependent ionization yield of the molecule [4] as follows: The ionization signal over the time delay, $M(t)$, is the convolution of the molecular axis distribution $A(\theta, t)$ and the angular dependence of the ionization yield, $S(\theta)$:

$$M(t) \propto \int_0^\pi S(\theta) A(\theta, t) \sin \theta \, d\theta. \tag{1}$$

A. Retrieval method

Now we turn to the retrieval procedure to get the angular dependence of electron rescattering based on the measured time-domain signals. Since NSDI can be treated as a two-step process with the first step of single ionization and the second step of electron rescattering, the angular dependence of NSDI can be written as $S_{NSDI}(\theta) = S_{SI}(\theta) S_{RES}(\theta)$, where S_{NSDI}, S_{SI}, and S_{RES} are the angular dependencies of double ionization, single ionization, and electron rescattering [23]. Based on Eq. (1), we first obtained the angular dependence $[S(\theta)]$ of single- and double-ionization channels from the measured time-domain yields $[M(t)]$ and the *in situ* measured $A(\theta, t)$. For the ionization process, since the ionization angular dependence function $S(\theta)$ is determined by the shapes of the involved molecular orbitals, we preset it with a polynomial

trigonometric function with unknown coefficients according to the symmetry of the involved molecular orbital. Through a fitting procedure we minimize the difference between the reconstructed and measured $M(t)$ and retrieve the coefficients and therewith the ionization angular dependence function $S(\theta)$ for the single- and double-ionization channels. More details can be found in the Appendix. In the end, with the obtained $S_{SI}(\theta)$ and $S_{NSDI}(\theta)$, the angular dependence of electron rescattering, $S_{RES}(\theta)$, can be retrieved. With this procedure, we retrieved the angular dependence of electron rescattering for the two NSDI channels: Channel 2, nondissociative, and channel 5, dissociative.

B. Rescattering-induced nondissociative double ionization

First, we focus on the nondissociative NSDI, channel 2, which is induced by electron rescattering following channel 1. The yields of channel 1 over pulse delay, depicted in Fig. 2(a), show a flat hump with a shallow dip around 21 ps and minimal values at perpendicular alignment which indicates that ionization takes place predominantely from the highest occupied molecular orbital (HOMO) [36]. Stable CO_2^{2+} in channel 2 is produced by removal of two electrons from the HOMO [37], which leads to similar behavior of the time-domain signals as compared to channel 1 but with a deeper dip at 21 ps [Fig. 2(a)]. As depicted in Fig. 1(b) the HOMO of CO_2 possesses a π_g symmetry with a butterfly shape; therefore, we set

$$S_{SI}(\theta) = \cos^n(\theta - \theta_m) + \cos^n(\theta + \theta_m), \tag{2}$$

where n defines the width of the four leaves and θ_m represents the angle at the maximum signal [4]. With this function, we fitted the measured signal $M(t)$ of channel 1 to obtain $S_{SI}(\theta)$ which yields $n = 7.4$ and $\theta_m = 37.5°$ (see Appendix). The retrieved maximum angle of $37.5°$ is close to $39°$ measured in the experiment by Oppermann *et al.* [23], but deviates from about $45°$ in three other previous experiments [4,38,39]. Our result is consistent with several theoretical studies which predict a maximum angle in the range of $36°$ to $40°$ [40–44]. The second step in NSDI to stable CO_2^{2+} is the emission of a second electron from the HOMO during electron rescattering. Using the same fitting function [Eq. (2)], we get $S_{NSDI}(\theta)$ from the measured signal $M(t)$ of channel 2 with $n = 50$ and $\theta_m = 49.0°$, which leads to a much narrower distribution than single ionization. The reconstructed time-domain ionization yields are depicted in Figs. 3(a) and 3(b), in which the fitted $M(t)$ curves achieve good agreement with the measured signals and well reproduce the dip structures around 21 ps in the measured yields. The retrieved angular dependence of single ionization [$S_{SI}(\theta)$, the dashed blue line] and second ionization [$S_{NSDI}(\theta)$, the dot-dashed red line] are presented in Fig. 3(c). We further retrieved the angular dependence of electron rescattering for the nondissociative NSDI which is plotted in Fig. 3(c) as the solid line with a peak at $51°$ and a much narrower distribution than that of single ionization. The angle is close to the result of Oppermann *et al.* which is $52°$ [23]. However, the retrieved angular distribution of electron rescattering in Ref. [23] is much broader than our result due to the fact that the influence from the alignment angular distribution was not ruled out in that work. In our approach, the molecular alignment
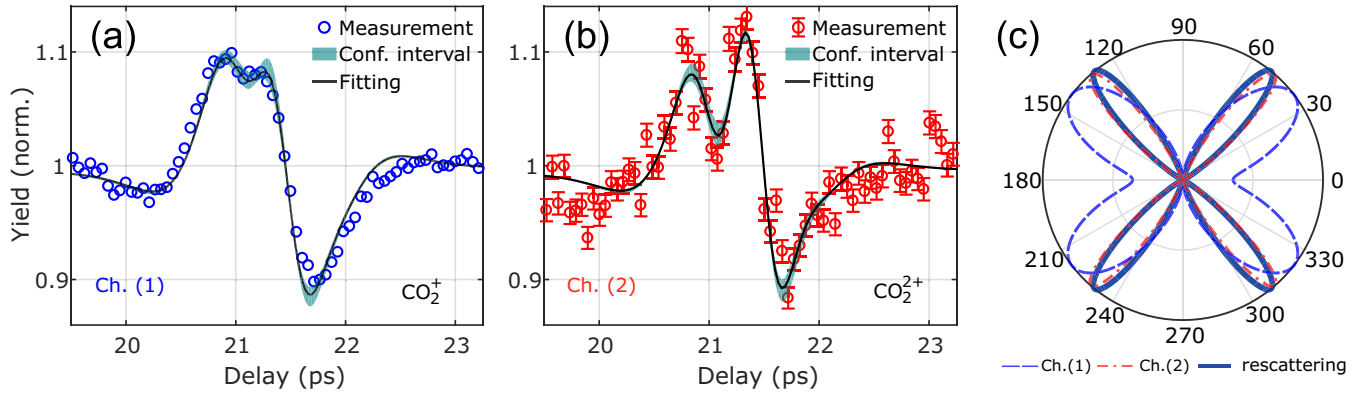
FIG. 3. Measured (circles) and fitted (solid black lines) ion yields for the nondissociative channels, (a) CO_2^+ and (b) CO_2^{2+}, as a function of time delay. The transparent areas around the solid lines are the fitting confidence interval with the range of the deviation 0.05. (c) Angular distributions of single ionization (dashed blue line), double ionization (dot-dashed red line), and electron rescattering during NSDI (solid bold line). The maximum angles of ionization and rescattering are located at $37.5°$, $49.0°$, and $51.0°$, respectively. The error bars of channel 1 in (a) are smaller than the circles.

distribution has been deconvoluted out from the retrieved angular distribution and thus the obtained angular distribution of electron rescattering is independent of the alignment quality and therewith free from systematic errors.

C. Rescattering-induced dissociative double ionization

Now we switch to the dissociative double ionization induced by electron rescattering, channel 5, which must involve different ionization dynamics than channel 2. Due to the small difference between the ionization potential of the HOMO and low-lying molecular orbitals, electrons in low-lying molecular orbitals can be released as well and make a significant contribution to strong-field ionization [23,45]. Ionization from low-lying valence molecular orbitals prepares the molecular cation in dissociative excited states. In the case of CO_2, such ionization will result in the observed dissociative channels 3 and 4. A further ionization step induced by electron rescattering will then bring the molecule into a dissociative excited state of CO_2^{2+} and will result in Coulomb explosion of the molecular ion (channel 5). There are several possible pathways to reach a dissociative state of CO_2^{2+}: first ionization from the HOMO (channel 1) followed by removal of the second electron from HOMO-1 or HOMO-2, or first ionization from HOMO-1 or HOMO-2 followed by removal of the second electron from the HOMO. For rescattering ionization, the impact energy of the first electron needs to be sufficient to overcome the binding energy of the second electron. The vertical energy to further remove an electron from the HOMO after single ionization is about 23.4 eV, while the vertical energy to reach the lowest dissociative electronic state of CO_2^{2+} is about 29 eV [46–49]. In our experiment with the laser peak intensity of 1.5×10^{14} W/cm^2, the cutoff energy of the rescattering electron is 28 eV which indicates that the most preferable ionization happens by removal of a HOMO electron during electron rescattering. Thus the measured dissociation of CO_2^{2+} (channel 5) originates dominantly from first removal of an electron from HOMO-1 or HOMO-2 (channels 3 and 4) and rescattering ionization from the HOMO.

Therefore, we can apply the retrieval procedure to obtain the angular dependence of electron rescattering in channel 5 based on the measured time-domain signals of channels 3–5. We used a fitting function of $S(\theta) = (1 - a)\cos^{n_1}(\theta) + a\sin^{n_2}(\theta)$ with contributions from HOMO-1 (second term) and HOMO-2 (first term) for channels 3 and 4, which yields the fitting parameters (n_1, a, n_2) of $(3.26, 0, -)$ for channel 3 and $(2.97, 0.11, 6.6)$ for channel 4 (see Appendix). The fitting parameter $a = 0$ for channel 3 indicates that the ionization for the dissociation channel 3 is dominated by removal of an electron from HOMO-2. Channel 4 has a dominant contribution from HOMO-2 but with about 11% contributions from HOMO-1. Further, we used the information of channels 3 and 4 as the first step of dissociative NSDI (channel 5). For the angular dependence of channel 5, we used the fitting function as in Eq. (2) and obtained $n = 25.5$ and $\theta_m = 45.8°$. Figures 4(a)–4(c) show the fitting results of measured time-domain signals. Since the first ionization step of dissociative NSDI is a combination of channels 3 and 4, we calculate the angular dependence of electron rescattering as $S_{RES}(\theta) = S_{CH5}(\theta)/[\alpha S_{CH3} + \beta S_{CH4}(\theta)]$ with α and β the channel strength of channels 3 and 4. The resulting angular distribution of electron rescattering to dissociative double ionization is plotted in Fig. 4(d) with a narrow distribution that peaks at $55°$. The peak angle slightly deviates from that of nondissociative NSDI ($51°$), which implies that the angular dependence of electron rescattering is affected by the ionic state populated by the first step of ionization even though the electron-impact ionization happens from the same molecular orbital, i.e., the HOMO.

IV. CONCLUSION AND OUTLOOK

In summary, we demonstrated a time-domain method to quantitatively retrieve the angular dependence of electron rescattering from nondissociative and dissociative NSDI of molecules. We demonstrate this approach by performing measurements and retrievals using the CO_2 molecule as an example. In the retrieval procedure, we used the channel-resolved ionization signals in combination with the *in situ*
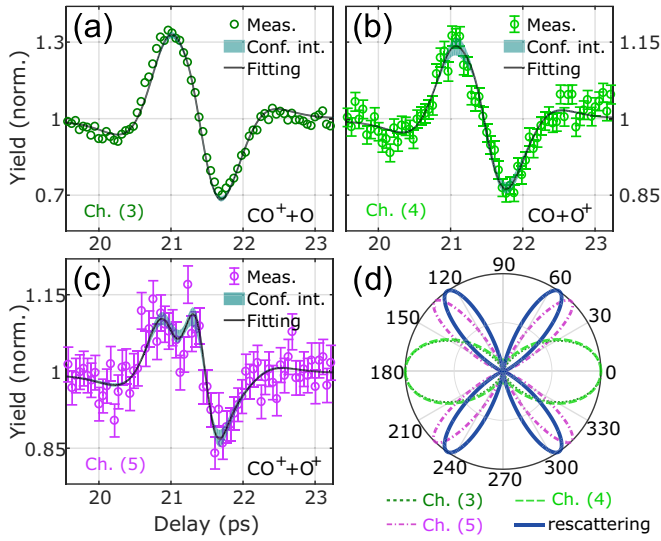
FIG. 4. (a–c) The same as Figs. 3(a) and 3(b) but for the three dissociative channels: channel 3, $CO_2^+ \rightarrow CO^+ + O$ (dark green); channel 4, $CO_2^+ \rightarrow CO + O^+$ (light green); and channel 5, $CO_2^{2+} \rightarrow CO^+ + O^+$ (purple), respectively. (d) Retrieved angular distributions of the three dissociative channels and electron rescattering during the dissociative NSDI (channel 5). The maximum positions of the dot-dashed purple line and solid bold line are located at $45.8°$ and $55.0°$, respectively. The error bars for channel 3 in (a) are smaller than the circle size.

measured angular distribution of the field-free molecular alignment from the coincidence measurements with a reaction microscope, such that the effect of molecular alignment quality can be excluded in the retrieved result. Furthermore, the presented method can be extended to the retrieval of three-dimensional angular dependence of ionization and electron rescattering with the measured three-dimensional momentum vectors of resulting particles from the strong-field interaction of molecules using a reaction microscope.

ACKNOWLEDGMENTS

APPENDIX: FITTING PROCEDURE

The ionization yield as a function of time delay is the convolution of the molecular alignment distribution and the ionization angular probability: $M(t) \propto \int_0^\pi S(\theta) A(\theta, t) \sin(\theta) \, d\theta$. The ionization yield as a function of time delay is measured directly in the experiment which is defined as $M_{\mathrm{mea}}(t)$ and shown in Fig. 2. The molecular axis distribution, $A(\theta, t)$, is determined from the Coulomb explosion of channel 5 at each time delay. Our goal is to retrieve the angular dependence of ionization, $S(\theta)$, based on $M_{\mathrm{mea}}(t)$ and $A(\theta, t)$.

Comparing to directly deconvoluting Eq. (1) with the measured ion yield and the alignment distribution, a more practical and robust way is to obtain $S(\theta)$ through a fitting procedure. The minimum deviation between the fitted $M(t)$ [marked as $M_{\mathrm{cal}}(t)$] and the target $M_{\mathrm{mea}}(t)$ can be achieved by
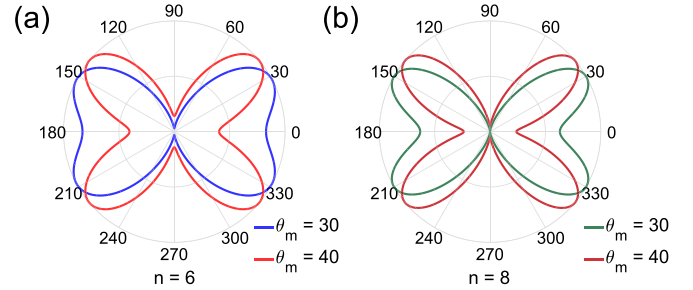

FIG. 5. The trial function $S(\theta)$ with different parameters: n and θ_m.

scanning the value of the parameters which are used to define, $S(\theta)$. We determine $S(\theta)$ when the deviation reaches its global minimum. The fitting procedure can be separated into three steps:

(1) Set a trial function of $S(\theta)$ based on the symmetry of the molecular orbitals with unknown fitting parameters.

(2) Calculate $M_{\mathrm{cal}}(t)$ as a function of the unknown fitting parameters with the measured $A(\theta, t)$ using Eq. (1).

(3) Find the global minimum of the deviation between $M_{\mathrm{mea}}(t)$ and $M_{\mathrm{cal}}(t)$ as a function of the fitting parameters.

As an example, we show the fitting procedure for single ionization, channel 1, in the following three steps:

(1) The electron removed during single ionization of CO_2 is mainly emitted from the HOMO, so the trial function $S(\theta)$ for single ionization can be set as $S_{\mathrm{SI}}(\theta) = \cos^n(\theta - \theta_m) + \cos^n(\theta + \theta_m)$, where n controls the width of the leaves and θ_m controls the angle at the maximum signal. If the molecular symmetry is unknown, the angular dependence can be set as a sum of weighted triangular functions. Figure 5 shows examples of trial functions $S(\theta)$ with different parameters.

(2) By using the trial $S(\theta)$ with different parameters, we can get the different shapes of $M_{\mathrm{cal}}(t)$ calculated using Eq. (1), as shown by Fig. 6.

(3) The deviation is calculated by the sum of the difference square of $M_{\mathrm{mea}}(t)$ and $M_{\mathrm{cal}}(t)$ at every time point: Deviation $= \sum_{i=1}^N [M_{\mathrm{mea}}(t_i) - M_{\mathrm{cal}}(t_i)]^2$. Figure 7 shows the deviation distribution over the two parameters. The minimum value of the deviation is 1.11 with the corresponding parameters $n = 7.4$ and $\theta_m = 37.5°$, shown by the solid red circle in Fig. 7.

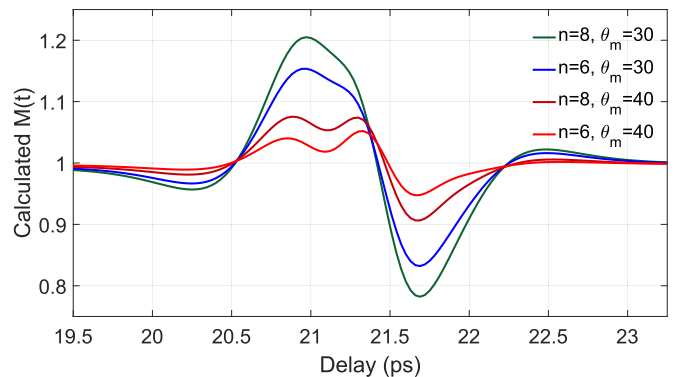FIG. 6. The shapes of $M_{\mathrm{cal}}(t)$ calculated by using the angular dependence corresponding to the four cases in Fig. 5.
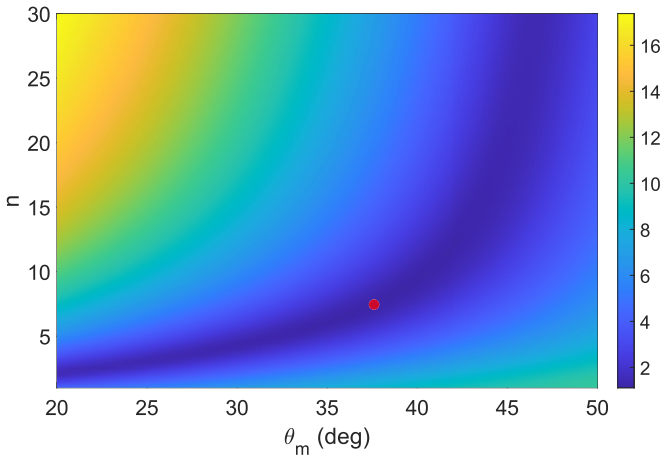
FIG. 7. The distribution of the deviation between $M_{\text{mea}}(t)$ and $M_{\text{cal}}(t)$ of the single ionization over the two parameters, n and θ_m. The red circle is the position of the minimum of the deviation.

As shown in Fig. 3(a) in the main text, the $M_{\text{cal}}(t)$ for the single-ionization channel agrees well with $M_{\text{mea}}(t)$. The blue curve in Fig. 3(c) is the corresponding retrieved angular dependence of single ionization.

The following table summarizes the trial functions and fitting results of the five channels. Note that n_2 is meaningless because $a=0$ for channel 3.

Channel	Trial functions	Fitting results
1	$\cos^n(\theta - \theta_m) + \cos^n(\theta + \theta_m)$	$(7.4, 37.5°)$
2	$\cos^n(\theta - \theta_m) + \cos^n(\theta + \theta_m)$	$(50, 49.0°)$
3	$(1-a)\cos^{n_1}(\theta) + a\sin^{n_2}(\theta)$	$(3.26, 0, -)$
4	$(1-a)\cos^{n_1}(\theta) + a\sin^{n_2}(\theta)$	$(2.97, 0.11, 6.6)$
5	$\cos^n(\theta - \theta_m) + \cos^n(\theta + \theta_m)$	$(25.5, 45.8°)$

[1] M. Meckel, D. Comtois, D. Zeidler, A. Staudte, D. Pavicic, H. C. Bandulet, H. Pepin, J. C. Kieffer, R. Dorner, D. M. Villeneuve, and P. B. Corkum, Science **320**, 1478 (2008).

[2] C. I. Blaga, J. Xu, A. D. DiChiara, E. Sistrunk, K. Zhang, P. Agostini, T. A. Miller, L. F. DiMauro, and C. D. Lin, Nature (London) **483**, 194 (2012).

[3] S. G. Walt, N. Bhargava Ram, M. Atala, N. I. Shvetsov-Shilovski, A. von Conta, D. Baykusheva, M. Lein, and H. J. Worner, Nat. Commun. **8**, 15651 (2017).

[4] D. Pavicić, K. F. Lee, D. M. Rayner, P. B. Corkum, and D. M. Villeneuve, Phys. Rev. Lett. **98**, 243001 (2007).

[5] T. Kanai, S. Minemoto, and H. Sakai, Nature (London) **435**, 470 (2005).

[6] Z. Diveki, A. Camper, S. Haessler, T. Auguste, T. Ruchon, B. Carré, P. Salières, R. Guichard, J. Caillat, A. Maquet, and R. Taïeb, New J. Phys. **14**, 023062 (2012).

[7] H. Yun, S. J. Yun, G. H. Lee, and C. H. Nam, J. Phys. B: At. Mol. Opt. Phys. **50**, 022001 (2017).

[8] A. S. Alnaser, C. M. Maharjan, X. M. Tong, B. Ulrich, P. Ranitovic, B. Shan, Z. Chang, C. D. Lin, C. L. Cocke, and I. V. Litvinyuk, Phys. Rev. A **71**, 031403(R) (2005).

[9] J. Mikosch, A. E. Boguslavskiy, I. Wilkinson, M. Spanner, S. Patchkovskii, and A. Stolow, Phys. Rev. Lett. **110**, 023004 (2013).

[10] D. Zeidler, A. Staudte, A. B. Bardon, D. M. Villeneuve, R. Dörner, and P. B. Corkum, Phys. Rev. Lett. **95**, 203003 (2005).

[11] H. V. S. Lam, S. Yarlagadda, A. Venkatachalam, T. N. Wangjam, R. K. Kushawaha, C. Cheng, P. Svihra, A. Nomerotski, T. Weinacht, D. Rolles, and V. Kumarappan, Phys. Rev. A **102**, 043119 (2020).

[12] X. Xie, K. Doblhoff-Dier, H. Xu, S. Roither, M. S. Schöffler, D. Kartashov, S. Erattupuzha, T. Rathje, G. G. Paulus, K. Yamanouchi, A. Baltuška, S. Gräfe, and M. Kitzler, Phys. Rev. Lett. **112**, 163003 (2014).

[13] B. Wolter, M. G. Pullen, A. T. Le, M. Baudisch, K. Doblhoff-Dier, A. Senftleben, M. Hemmer, C. D. Schroter, J. Ullrich, T. Pfeifer, R. Moshammer, S. Grafe, O. Vendrell, C. D. Lin, and J. Biegert, Science **354**, 308 (2016).

[14] X. Xie, G. Jordan, M. Wickenhauser, and A. Scrinzi, J. Mod. Opt. **54**, 999 (2007).

[15] P. B. Corkum and F. Krausz, Nat. Phys. **3**, 381 (2007).

[16] F. Krausz and M. Ivanov, Rev. Mod. Phys. **81**, 163 (2009).

[17] M. Meckel, A. Staudte, S. Patchkovskii, D. M. Villeneuve, P. B. Corkum, R. Dorner, and M. Spanner, Nat. Phys. **10**, 594 (2014).

[18] C. Vozzi, M. Negro, F. Calegari, G. Sansone, M. Nisoli, S. De Silvestri, and S. Stagira, Nat. Phys. **7**, 822 (2011).

[19] B. Walker, B. Sheehy, L. F. DiMauro, P. Agostini, K. J. Schafer, and K. C. Kulander, Phys. Rev. Lett. **73**, 1227 (1994).

[20] C. Guo, M. Li, J. P. Nibarger, and G. N. Gibson, Phys. Rev. A **58**, R4271(R) (1998).

[21] E. Eremina, X. Liu, H. Rottke, W. Sandner, A. Dreischuh, F. Lindner, F. Grasbon, G. G. Paulus, H. Walther, R. Moshammer, B. Feuerstein, and J. Ullrich, J. Phys. B: At. Mol. Opt. Phys. **36**, 3269 (2003).

[22] B. Bergues, M. Kübel, N. G. Johnson, B. Fischer, N. Camus, K. J. Betsch, O. Herrwerth, A. Senftleben, A. M. Sayler, T. Rathje, T. Pfeifer, I. Ben-Itzhak, R. R. Jones, G. G. Paulus, F. Krausz, R. Moshammer, J. Ullrich, and M. F. Kling, Nat. Commun. **3**, 813 (2012).

[23] M. Oppermann, S. J. Weber, L. J. Frasinski, M. Y. Ivanov, and J. P. Marangos, Phys. Rev. A **88**, 043432 (2013).

[24] F. Schell, T. Bredtmann, C. P. Schulz, S. Patchkovskii, M. J. J. Vrakking, and J. Mikosch, Sci. Adv. **4**, 5 (2018).

[25] R. Dörner, V. Mergel, O. Jagutzki, L. Spielberger, J. Ullrich, R. Moshammer, and H. Schmidt-Böcking, Phys. Rep. **330**, 95 (2000).

[26] J. Ullrich, R. Moshammer, A. Dorn, R. Dörner, L. P. H. Schmidt, and H. Schmidt-Böcking, Rep. Prog. Phys. **66**, 1463 (2003).

[27] X. Xie, S. Roither, D. Kartashov, E. Persson, D. G. Arbó, L. Zhang, S. Gräfe, M. S. Schöffler, J. Burgdörfer, A. Baltuška, and M. Kitzler, Phys. Rev. Lett. **108**, 193004 (2012).

[28] L. Cai, J. Marango, and B. Friedrich, Phys. Rev. Lett. **86**, 775 (2001).

[29] A. Rudenko, V. Makhija, A. Vajdi, T. Ergler, M. Schürholz, R. K. Kushawaha, J. Ullrich, R. Moshammer, and V. Kumarappan, Faraday Discuss. **194**, 463 (2016).

[30] H. Stapelfeldt and T. Seideman, Rev. Mod. Phys. **75**, 543 (2003).

[31] A. S. Alnaser, X. M. Tong, T. Osipov, S. Voss, C. M. Maharjan, B. Shan, Z. Chang, and C. L. Cocke, Phys. Rev. A **70**, 023413 (2004).

[32] S. Larimian, S. Erattupuzha, S. Mai, P. Marquetand, L. González, A. Baltuška, M. Kitzler, and X. Xie, Phys. Rev. A **95**, 011404(R) (2017).

[33] J. Ortigoso, M. Rodrıguez, M. Gupta, and B. Friedrich, J. Chem. Phys. **110**, 3870 (1999).

[34] T. N. Olney, N. Cann, G. Cooper, and C. Brion, Chem. Phys. **223**, 59 (1997).

[35] G. Herzberg, *Electronic Spectra and Electronic Structure of Polyatomic Molecules* (Krieger, Malabar, FL, 1991), Vol. 2.

[36] A.-T. Le, X.-M. Tong, and C.-D. Lin, Phys. Rev. A **73**, 041402(R) (2006).

[37] S. Erattupuzha, S. Larimian, A. Baltuška, X. Xie, and M. Kitzler, J. Chem. Phys. **144**, 024306 (2016).

[38] I. Thomann, R. Lock, V. Sharma, E. Gagnon, S. T. Pratt, H. C. Kapteyn, M. M. Murnane, and W. Li, J. Phys. Chem. A **112**, 9382 (2008).

[39] C. Marceau, J. B. Bertrand, P. Peng, H. J. Wörner, P. B. Corkum, and D. M. Villeneuve, J. Phys. B: At. Mol. Opt. Phys. **53**, 084006 (2020).

[40] S.-F. Zhao, C. Jin, A.-T. Le, T. F. Jiang, and C. D. Lin, Phys. Rev. A **80**, 051402(R) (2009).

[41] S. Petretti, Y. V. Vanne, A. Saenz, A. Castro, and P. Decleva, Phys. Rev. Lett. **104**, 223001 (2010).

[42] R. Murray, M. Spanner, S. Patchkovskii, and M. Y. Ivanov, Phys. Rev. Lett. **106**, 173001 (2011).

[43] S.-K. Son and Shih-I Chu, Phys. Rev. A **80**, 011403(R) (2009).

[44] M. D. Śpiewanowski and L. B. Madsen, Phys. Rev. A **91**, 043406 (2015).

[45] X. Xie, S. Roither, M. Schöffler, E. Lötstedt, D. Kartashov, L. Zhang, G. G. Paulus, A. Iwasaki, A. Baltuška, K. Yamanouchi, and M. Kitzler, Phys. Rev. X **4**, 021005 (2014).

[46] R. Hall, L. Avaldi, G. Dawber, A. McConkey, M. MacDonald, and G. King, Chem. Phys. **187**, 125 (1994).

[47] L. S. Wang, J. Reutt, Y. Lee, and D. Shirley, J. Electron Spectrosc. Relat. Phenom. **47**, 167 (1988).

[48] M. Hochlaf, F. Bennett, C. Gilberte, and P. Rosmus, J. Phys. B: At. Mol. Opt. Phys. **31**, 2163 (1998).

[49] A. N. Zavilopulo, F. F. Chipev, and O. B. Shpenik, Tech. Phys. **50**, 402 (2005).